

Supporting Information

FROM BIOMASS TO SUGAR ALCOHOLS: PURIFICATION OF WHEAT BRAN HYDROLYSATES USING BORONIC ACID CARRIERS FOLLOWED BY HYDROGENATION OF SUGARS OVER RU/H-ZSM-5

Nuria Sánchez-Bastardo[†], Irina Delidovich[‡], and Esther Alonso^{*†}

[†]High Pressure Processes Group, Chemical Engineering and Environmental Technology Department, University of Valladolid, Dr. Mergelina s/n, Valladolid, 47011, Spain.

[‡]Chair of Heterogeneous Catalysis and Chemical Technology, RWTH Aachen University, Worringerweg 2, Aachen, 52074, Germany.

* Corresponding author. E-mail address: ealonso@iq.uva.es

Number of pages: 21

Number of figures: 10

Number of tables: 7

INTRODUCTION

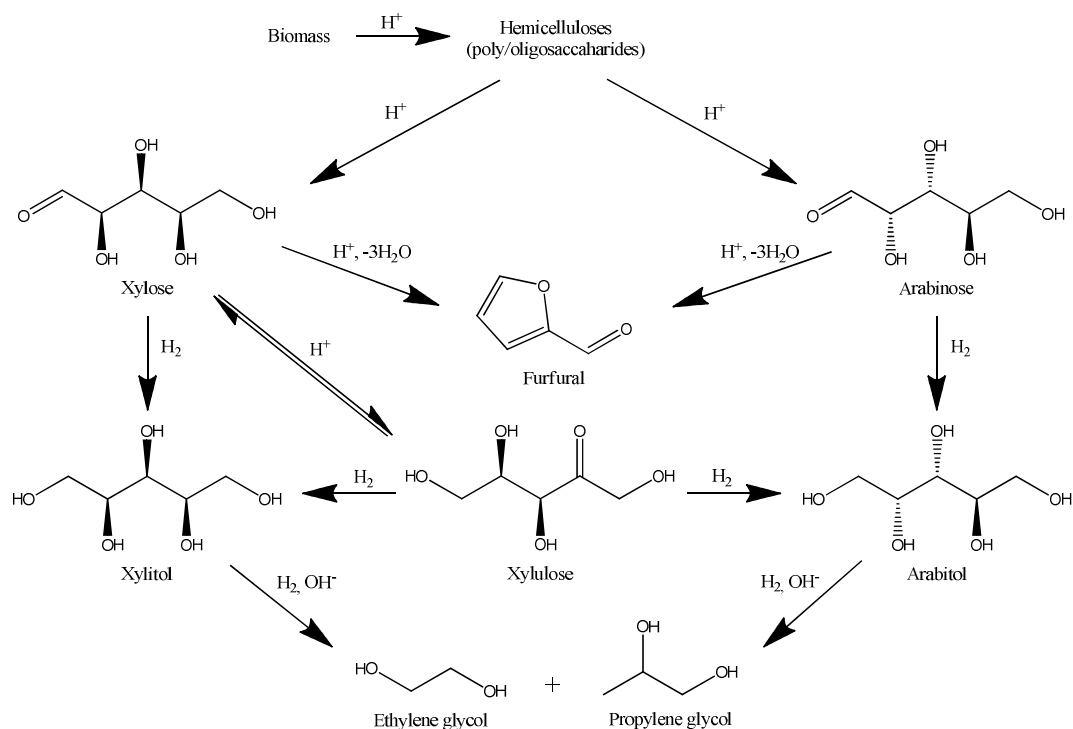


Figure S1. Chemical production of sugar alcohols from biomass with possible side reactions. Adapted from literature.¹⁻⁴

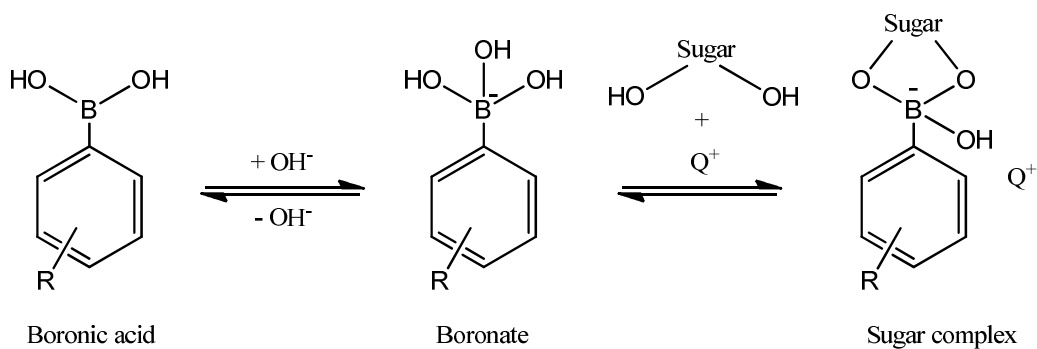


Figure S2. Mechanism of complexation of sugars by anionic extraction.

EXPERIMENTAL SECTION

Table S1. Composition of wheat bran hydrolysate.

Component	Concentration (ppm)
Sugars	
Xyl	5594 ± 53
Ara	2829 ± 39
Glc	767 ± 21
Degradation products	
Furfural	275 ± 19
Proteins	
Inorganic elements	
Mg	62 ± 2
Ca	13 ± 1
K	69 ± 3
S	4 ± 1

Table S2. Operating conditions of the different HPLC columns used in this work.

Parameter	HPLC Column		
	Supelcogel Pb	SH1011	SC1211
Compounds analyzed	Sugars	Degradation products	Sugar alcohols
Furnace temperature (°C)	85	50	90
Detector temperature (°C)	35	35	35
Mobile phase	Milli-Q water	H ₂ SO ₄ 0.01 N in Milli-Q water	H ₂ O/CH ₃ CN (65/35 v/v)
Flow rate (mL min ⁻¹)	0.5	0.8	0.5
Detector	RI	RI and UV-Vis (254 nm for 5-HMF and 260 nm for furfural)	RI

Calculations

Extraction and back-extraction yields:

$$\% \text{ Extraction yield}_i = \frac{m_{i,0} - m_{i,E}}{m_{i,0}} \times 100 \quad (\text{Eq. S1})$$

$$\% \text{ Back-extraction yield}_i = \frac{m_{i,BE}}{m_{i,0} - m_{i,E}} \times 100 \quad (\text{Eq. S2})$$

where $m_{i,0}$, $m_{i,E}$ and $m_{i,BE}$ are the amounts of the component i in the initial phase and in the aqueous phases after extraction and back-extraction, respectively.

Conversion of sugars, yield and selectivity into the corresponding alcohols in the hydrogenation experiments:

$$\% \text{ Sugar conversion} = \frac{n_{\text{sugar},0} - n_{\text{sugar},f}}{n_{\text{sugar},0}} \times 100 \quad (\text{Eq. S3})$$

$$\% \text{ Pentitols yield} = \frac{n_{\text{pentitols},f}}{n_{\text{C5 sugars},0}} \times 100 \quad (\text{Eq. S4})$$

$$\% \text{ Pentitols selectivity} = \frac{n_{\text{pentitols},f}}{n_{\text{C5 sugars},0} - n_{\text{C5 sugars},f}} \times 100 \quad (\text{Eq. S5})$$

$$\% \text{ Sorbitol yield} = \frac{n_{\text{sorbitol},f}}{n_{\text{glucose},0}} \times 100 \quad (\text{Eq. S6})$$

$$\% \text{ Sorbitol selectivity} = \frac{n_{\text{sorbitol},f}}{n_{\text{glucose},0} - n_{\text{glucose},f}} \times 100 \quad (\text{Eq. S7})$$

where $n_{\text{sugar},0}$ and $n_{\text{sugar},f}$ are the moles of each sugar before and after the hydrogenation reaction, respectively; $n_{\text{C5 sugars},0}$ and $n_{\text{C5 sugars},f}$ are the initial and final moles of xylose + arabinose, respectively; $n_{\text{glucose},0}$ and $n_{\text{glucose},f}$ are the initial and final moles of glucose, respectively; $n_{\text{pentitols},f}$ are the moles of xylitol + arabitols formed from xylose + arabinose; and $n_{\text{sorbitol},f}$ are the moles of sorbitol formed from glucose.

RESULTS AND DISCUSSION

X-Ray Diffraction (XRD)

The diffraction peaks in the spectrum at $2\theta = 42.1^\circ$ and 44.0° demonstrate the presence of Ru^0 on Ru/H-ZSM-5 (Figure S3). These reflections are assigned to the (100) and (002) diffraction planes of bulk hexagonal Ru^0 particles (JCPDS-ICDD card No. 06-0663).⁵ The low intensity of the diffraction peaks is probably due to the low metal loading and high dispersion of Ru^0 particles onto the support.⁶

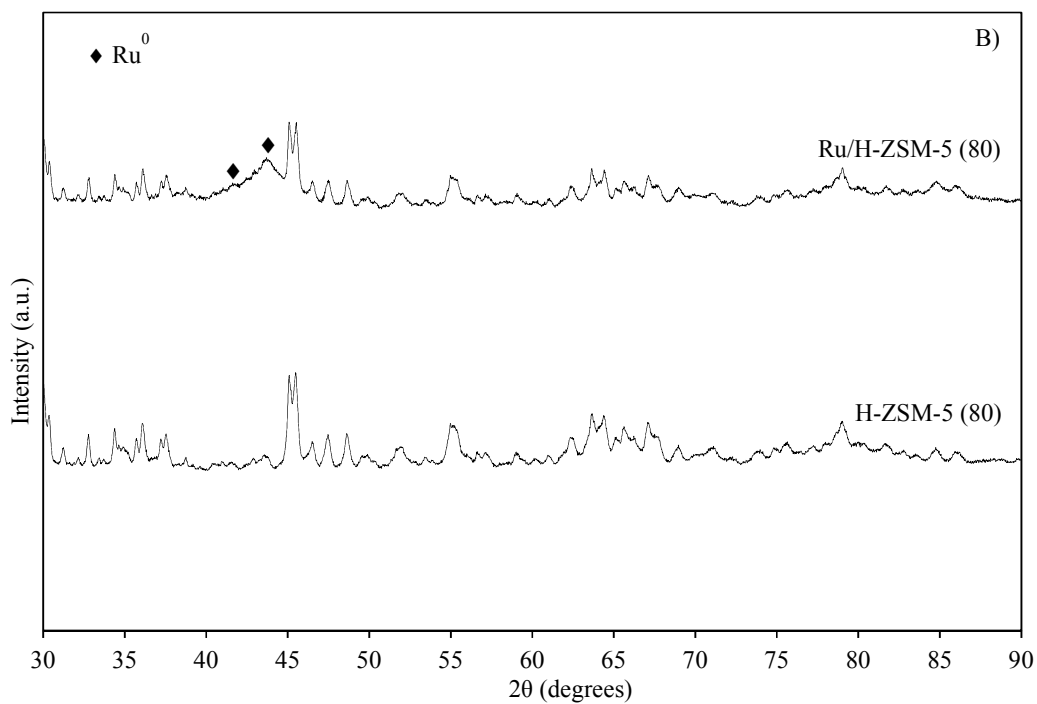
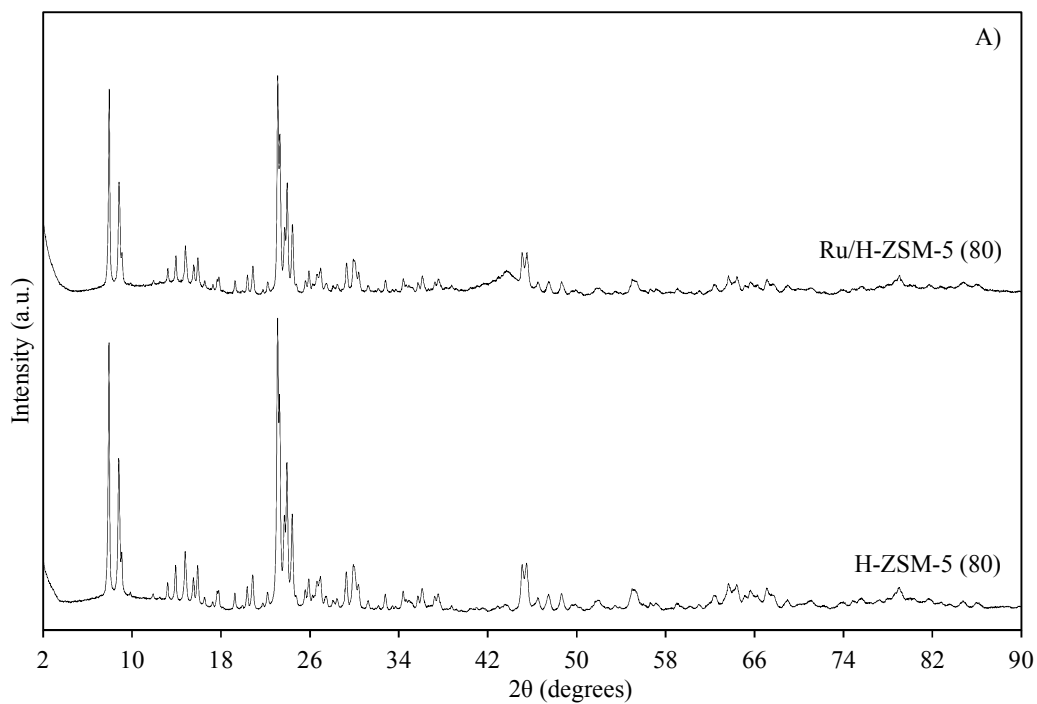


Figure S3. XRD patterns of H-ZSM-5 and reduced Ru/H-ZSM-5. A) 2° - 90° and B) expanded region from 30° - 90 °.

Nitrogen adsorption-desorption isotherms

Figure S4A displays type I isotherms, typical of microporous materials which exhibit a sharp increase of nitrogen sorption at very low partial pressures ($P/P_0 \leq 0.01$) due to the filling of ultramicropores with a width of two-three molecular diameters, which is governed by the gas – solid interactions.⁷ The pore filling process of supermicroporous occurs in the range of relative pressure $P/P_0 = 0.01-0.15$ ⁷ and the rise observed at $P/P_0 > 0.95$ is related to nitrogen condensation in the void volume between the particles.⁸ H-ZSM-5 and Ru/H-ZSM-5 display a slight H4 hysteresis loop.⁹ This kind of hysteresis is often associated with narrow slit-like pores, but in the case of type I isotherms is indicative of a microporous structure with some contribution of mesopores.^{7, 8, 10, 11} However, the pore size distribution (PSD) (Figure S4B) shows basically a unimodal microporous distribution centered at approximately 0.67 nm for both solids. A slight shoulder but also in the micropore region was observed. Therefore, the small hysteresis loop and the narrow pore size distribution suggests that mesoporosity in H-ZSM-5 and Ru/H-ZSM-5 is very low. Besides mesoporosity, several authors have attributed the hysteresis at relatively high pressures ($P/P_0 \geq 0.45$) to zeolites with low aluminum content, as in the case of H-ZSM-5 with a $\text{SiO}_2/\text{Al}_2\text{O}_3$ ratio of 80.¹²⁻¹⁶

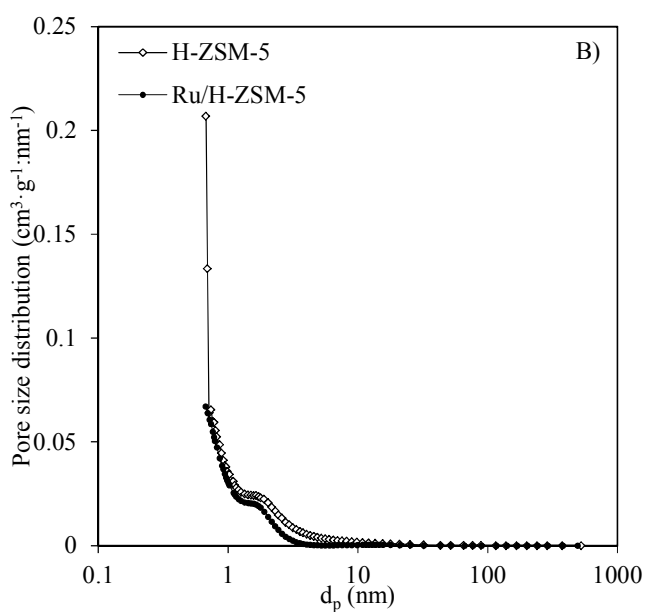
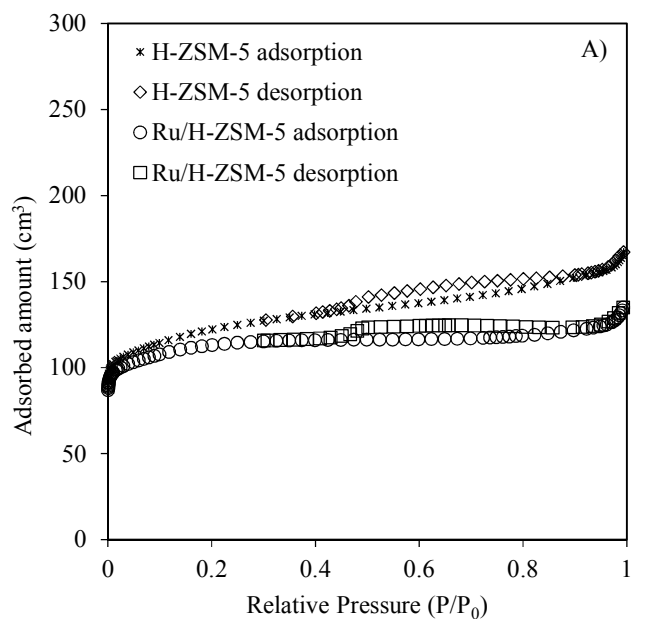


Figure S4. A) Nitrogen adsorption-desorption isotherms and B) pore size distributions (PSD) of H-ZSM-5 and Ru/H-ZSM-5.

Table S3. Textural properties of H-ZSM-5 and Ru/H-ZSM-5.

Catalyst	Ru ^a (%)	Specific Surface Area ^b (m ² g ⁻¹)	V _{pore} ^c (cm ³ g ⁻¹)	d _{pore} ^c (nm)
H-ZSM-5	-	562	0.26	0.67
Ru/H-ZSM-5	2.0 ± 0.3	515	0.21	0.67

^a Determined by ICP-AES

^b Determined by Langmuir model

^c Determined by Horvath-Kawazoe method

Recovery of sugars from model mixtures

Prior to the purification of hydrolysates, the extractability of C5 sugars from model mixtures in a phosphate buffer at pH 7.5 was studied following the scheme represented in Figure 1. Xylose and arabinose were chosen for the investigation of model mixtures since they are the major saccharides in the hydrolysates obtained from wheat bran (Table S1).

First, two different boronic acids, namely PBA and HMPBA, were tested. The results of the experiments to compare the efficiency of the extraction by PBA and HMPBA are shown in Figure S5. For the same boronic acid concentration, the amount of sugars extracted with HMPBA was higher than with PBA. In a previous work, HMPBA has also demonstrated to be more efficient than PBA for the extraction of saccharides.¹⁷ The complexation constants of HMPBA with sugars are higher than the corresponding to PBA-sugars. This is related to a lower pK_a of HMPBA and the formation of an intrinsic hydrogen bond between HMPBA and saccharides.¹⁷⁻¹⁹ As expected, a higher concentration of boronic acid enables a higher amount of sugars extracted into the organic phase. Additionally, xylose and arabinose were extracted basically in the same proportion, which is due to the similar complexation constants of both sugars with boronic acids.^{20, 21} The back-extraction of the sugars was performed by an acidic solution of 0.25 M H₂SO₄. In all the cases, 100% of both sugars was recovered since the complexes are no longer stable under acidic conditions.

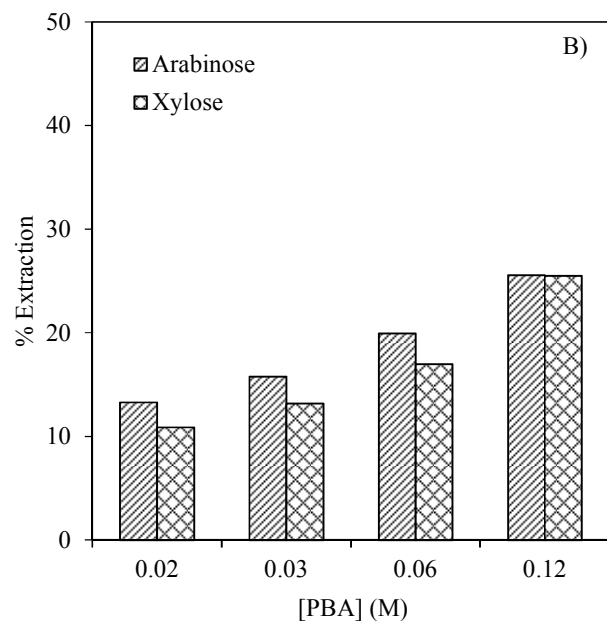
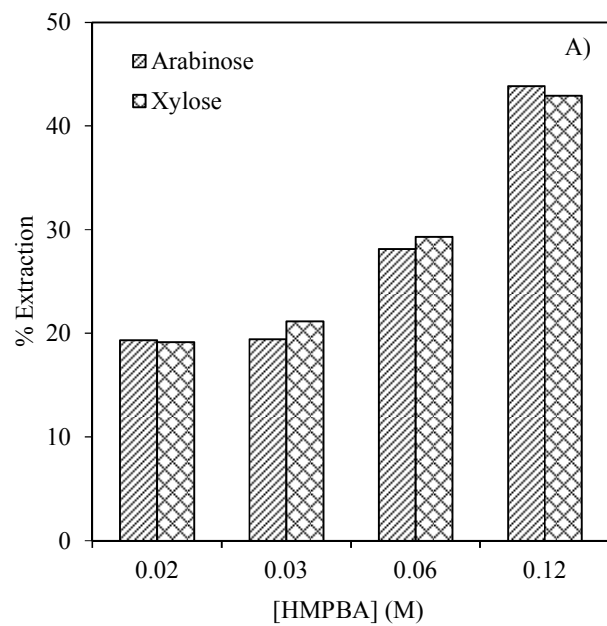


Figure S5. Extraction of arabinose and xylose with different concentrations of boronic acid: A) with HMPBA and B) with PBA.

Prior to the extraction of sugars, the organic phase was pretreated with a phosphate buffer at a pH₀ 7.5. The preactivation of the organic phase was demonstrated to be very important in previous studies to improve the extraction of saccharides.^{17, 22} During this

pretreatment, the pH of the buffer phosphate slightly decreased due to the transfer of hydroxyl groups from the aqueous to the organic phase. These OH⁻ groups are the responsible for the ionization of boronic acid, which enables the formation of the complexes with sugars.

The feasibility of obtaining more concentrated sugar solutions after the back-extraction was also studied (Figure S6). To do so, the organic phase was saturated with sugars by performing several extractions. Each extraction was carried out by stirring the same organic phase with a new sugar solution every time. The amount of the extracted sugars was very similar for each of these successive runs. However, the initial concentration of xylose was higher than arabinose (imitating a real hydrolysate), resulting therefore in a greater amount of xylose in the organic phase than arabinose after each extraction (Figure S6A). The stripping of the sugars was performed with a solution 0.25 M H₂SO₄. Nevertheless, this acid concentration was not enough to recover all the sugars, but only around 60%. A higher H₂SO₄ concentration (0.50 M) was tested to improve the amount of the back-extracted sugars. In this case, the sugars were completely recovered into the acidic solution, which gave rise to a sugar solution ~2.4 times more concentrated than the initial (Figure S6B).

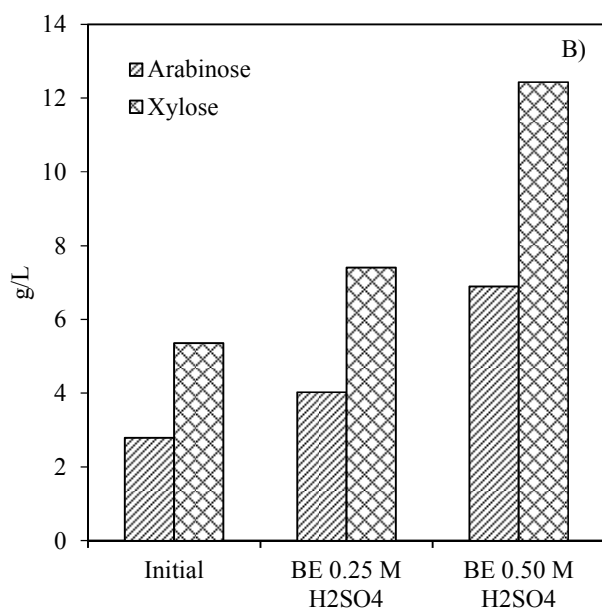
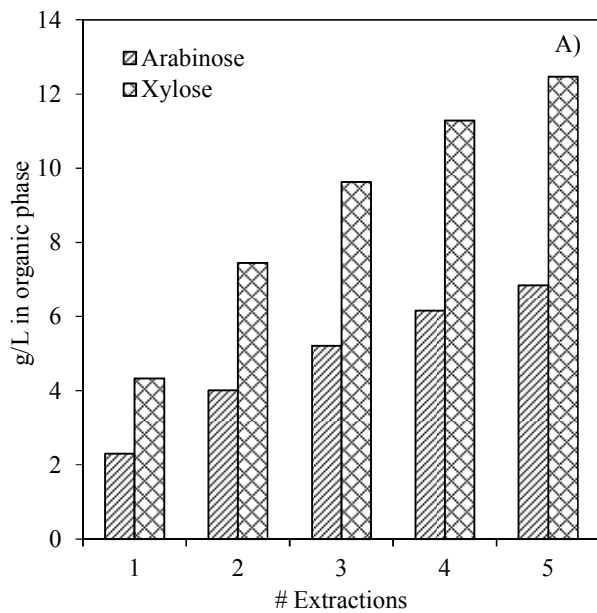


Figure S6. Concentration of sugar solutions by several extractions (Extraction with 0.5 M HMPBA): A) amount of sugars in the organic phase after each extraction and B) amount of sugars in the initial and final aqueous solutions after back-extraction with 0.25 M and 0.50 M H₂SO₄.

Purification of sugars from wheat bran hydrolysates

Inorganic elements

Table S4. Distribution of inorganic elements in the hydrolysate and in the aqueous phases after extraction and back-extraction.

Experiment		Inorganic elements (ppm)			
		Ca	Mg	K	S
Initial hydrolysate		13	62	69	4
0.25 M HMPBA	Extraction	12	63	70	5
	Back-extraction	ND	ND	ND	*
0.50 M HMPBA	Extraction	12	65	76	4
	Back-extraction	ND	ND	ND	*
0.75 M HMPBA	Extraction	12	67	71	4
	Back-extraction	ND	ND	ND	*
1-octanol	Extraction	13	62	69	3
	Back-extraction	ND	ND	ND	*
Aliquat® 336/1-octanol	Extraction	11	64	68	4
	Back-extraction	ND	ND	ND	*

* Sulfur detected after back-extraction corresponds to H₂SO₄ used for the recovery of sugars. This cannot correspond to S from the hydrolysate, since the S content after extraction is the same as in the initial solution.

Lignin derivatives

Table S5. Composition of the final aqueous phase after back-extraction and back-extraction + treatment with Amberlyst® 15 and Amberlite® IRA-96.

Experiment		% g C/TOC			
		Sugars	Furfural	Proteins	Not identified
0.25 M HMPBA	Back-extraction	70	1	ND	29
	Back-extraction + Resins	90	1	ND	8
0.50 M HMPBA	Extraction	70	1	ND	30
	Back-extraction + Resins	90	1	ND	9
0.75 M HMPBA	Extraction	69	1	ND	30
	Back-extraction + Resins	88	1	ND	12

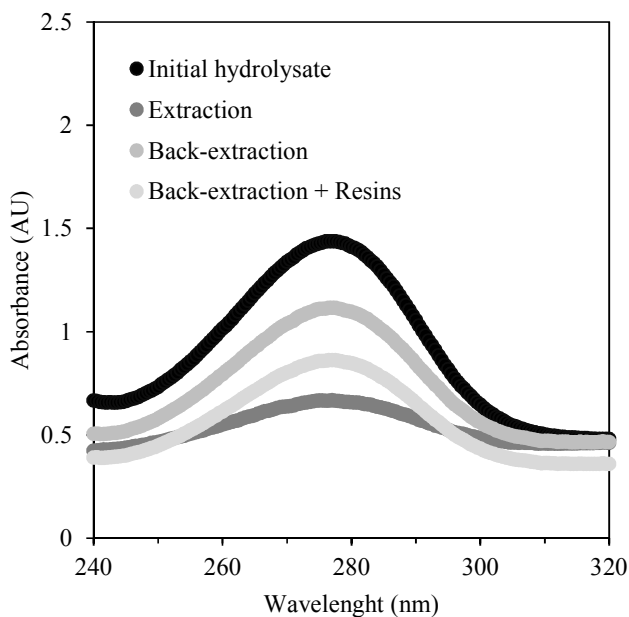


Figure S7. Absorbance spectra of a sample after extraction, back-extraction and before and after the treatment with Amberlyst® 15 and Amberlite® IRA-96.

Organic phase recycling

Table S6. Extraction of the different compounds using fresh and recycled organic phase.

Experiment	Extraction (%)				
	Glucose	Xylose	Arabinose	Furfural	Proteins
0.50 M HMPBA Fresh	53	79	82	80	34
0.50 M HMPBA Recycling	59	81	82	70	38

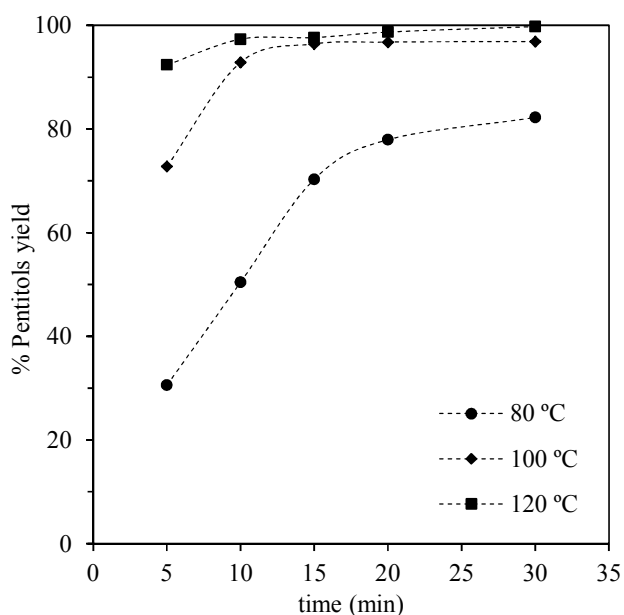
Hydrogenation of sugars model mixtures

First, we evaluated the activity of the Ru/H-ZSM-5 catalyst in the hydrogenation of sugars model mixtures into sugar alcohols. Ruthenium catalysts were chosen as they have demonstrated to be very active for hydrogenation of sugars in numerous works.²³⁻

³⁰ The experiments involved xylose and arabinose, as major components of the purified hydrolysate, but also glucose, as it is present after the purification. Different temperatures and catalyst loadings were tested. Figures S8 and S9 show the results corresponding to the hydrogenation of model mixtures composed of xylose, arabinose

and glucose. The yields of pentitols (xylitol + arabitol) and sorbitol were calculated according to the Eq. 4 and 6, respectively. Xylitol and arabitol may be formed from both xylose and arabinose (Figure S1), so the yield was evaluated in terms of total pentitols. Selectivity was in all the experiments $\sim 100\%$, which means that C5 sugars were converted only into xylitol and arabitol, and glucose into sorbitol. The formation of by-products (*e.g.* mannitol, levulinic acid, glycerol, ethylene glycol, propylene glycol or furfuryl alcohol) as reported in previous studies³¹ was not observed in any experiment. Furthermore, mass balances were above 98% in all the cases, corroborating the maximum selectivity into the alcohols of interest. Under the same experimental conditions, xylose and arabinose were hydrogenated more readily than glucose. This was previously reported by several authors.³¹⁻³³

First, the effect of temperature was investigated (Figure S8). The optimum temperature for the hydrogenation of xylose and arabinose was 100 °C, whereas 120 °C was the most suitable for the hydrogenation of glucose. Since we are interested in the maximization of pentitols and minimization of hexitols, 100 °C was chosen as optimum temperature.



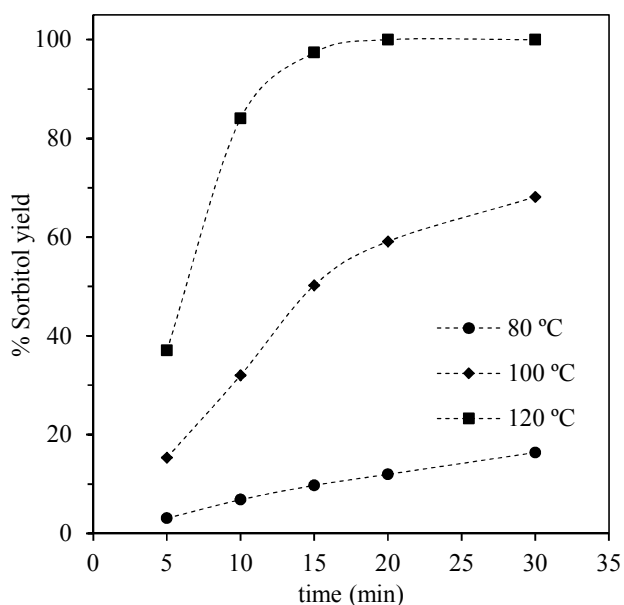


Figure S8. Effect of temperature in hydrogenation of sugars model mixtures. Conditions: xylose + arabinose + glucose, Ru/H-ZSM-5, 0.015 g Ru/g C, 100 °C, 50 bar H₂. A) Pentitols and B) sorbitol yield.

Different catalysts loadings were then tested (Figure S9). No sugars conversion and hence no alcohols production were observed in the blank experiments without catalyst. The maximum yield of pentitols was achieved at 100 °C after 10 minutes with a ratio of 0.015 grams of ruthenium per gram of total carbon in sugars. In the case of sorbitol, best results were obtained at 100 °C/15 min/0.06 g Ru g C⁻¹ or at 100 °C/30 min/0.03 g Ru g C⁻¹. In order to maximize the production of pentitols and minimize that of hexitols, our optimum conditions were selected at 100 °C/10 min/0.015 g Ru g C⁻¹.

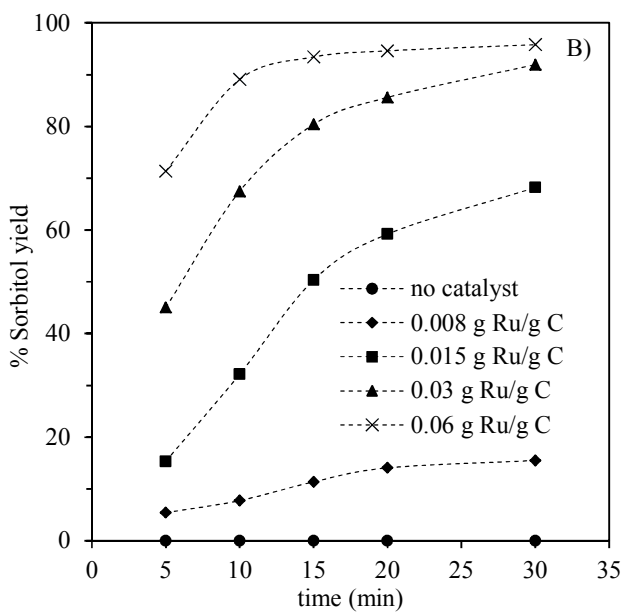
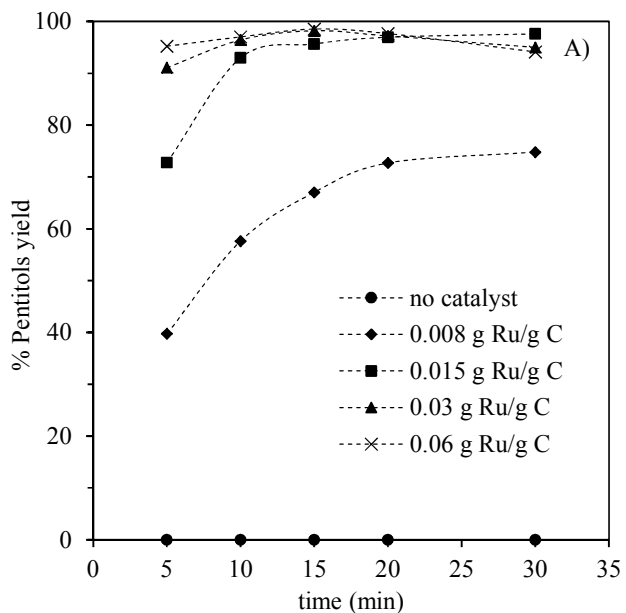


Figure S9. Influence of catalyst loading in hydrogenation of sugars model mixtures. Conditions: xylose + arabinose + glucose, Ru/H-ZSM-5, 100 °C, 50 bar H₂. A) Pentitols yield and B) sorbitol yield.

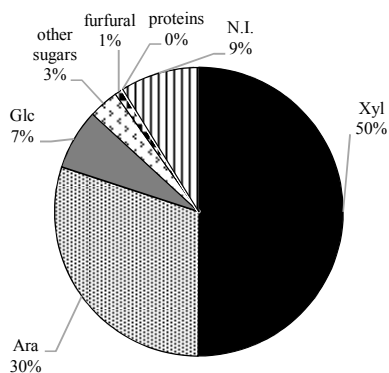


Figure S10. Composition of the purified hydrolysate based on carbon balance (lyophilized and at pH 7.0).

Table S7. Pretreatments performed in the initial wheat bran hydrolysate.

Pretreatment	Removed compounds	Non-removed compounds
Activated carbon	S	Ca, Mg, K, proteins
Dowex® Monosphere® MR-450 UPW	Ca, Mg, K	S, proteins
Activated carbon + Dowex® Monosphere® MR-450 UPW	S, Ca, Mg, K	Proteins
Anionic extraction + Back-extraction + Amberlyst® 15 + Amberlite® IRA-96	S, Ca, Mg, K, proteins	-

References

- Mishra, D. K.; Dabbawala, A. A.; Hwang, J-S. Ruthenium nanoparticles supported on zeolite Y as an efficient catalyst for selective hydrogenation of xylose to xylitol. *J. Mol. Catal. A-Chem.* **2013**, *376*, 63-70.
- Murzin, D. Y.; Murzina, E. V.; Tokarez, A.; Shcherban, N. D.; Wärna, J.; Salmi, T. Arabinogalactan hydrolysis and hydrolytic hydrogenation using functionalized carbon materials. *Catal. Today* **2015**, *257*, 169-176.
- Huang, Z.; Chen, J.; Jia, Y.; Liu, H.; Xia, C.; Liu, H. Selective hydrogenolysis of xylitol to ethylene glycol and propylene glycol over copper catalysts. *Appl. Catal. B-Environ.* **2014**, *147*, 377-386.

4. Kobayashi, H.; Komanoya, T.; Guha, S. K.; Hara, K.; Fukuoka, A. Conversion of cellulose into renewable chemicals by supported metal catalysts. *Appl. Catal. A-General* **2011**, *409-410*, 13-20.
5. Li, W.; Ye, L.; Long, P.; Chen, J.; Ariga, H.; Asakura, K.; Yuan, Y. Efficient Ru – Fe catalyzed selective hydrogenolysis of carboxylic acids to alcoholic chemicals. *RSC Adv.* **2004**, *4*, 29072.
6. Yao, G.; Wu, G.; Dai, W.; Guan, N.; Li, L. Hydrodeoxygenation of lignin-derived phenolic compounds over bi-functional Ru/H-Beta under mild conditions. *Fuel* **2015**, *150*, 175-183.
7. Cychosz, K. A.; Guillet-Nicolas, R.; García-Martínez, J.; Thommes, M. Recent advances in the textural characterization of hierarchically structures nanoporous materials. *Chem. Soc. Rev.* **2017**, *46*, 389-414.
8. Fu, X.; Sheng, X.; Zhou, Y.; Fu, Z.; Zhao, S.; Bu, X.; Zhang, C. Design of micro – mesoporous zeolite catalysts for alkylation. *RSC Adv.* **2016**, *6*, 50630-50639.
9. AlOthoman, Z. A. A Review: Fundamental aspects of silicate mesoporous materials. *Materials* **2012**, *5*, 2874-2902.
10. Peng, P.; Wang, Y.; Rood, M. J.; Zhang, Z.; Subhan, F.; Yan, Z.; Qin, L.; Zhang, Z.; Zhang, Z.; Gao, X. Effects of dissolution alkalinity and self-assembly on ZSM-5 based micro-/mesoporous composites: a study of the relationship between porosity, acidity, and catalytic performance. *CrystEngComm* **2015**, *17*, 3820-3828.
11. Beyer, H. K.; Nagy, J. B.; Karge, H. G.; Kiricsi, I; Ed. Catalysis by microporous materials. Volume 94, Studies in Surface Science and Catalysis, 1st ed., Elsevier Science, 1995.
12. Al-Thawabeia, R. A.; Hodali, H. A. Use of zeolite ZSM-5 for loading and release of 5-fluorouracil. *J. Chem.* **2015**, *2015*, Article ID 403597.

13. Cejka, J.; Van Bekkum, H.; Schueth, C.; Ed. Introduction to zeolite molecular sieves, 3rd ed., Elsevier Science: New York, 2007.
14. Hudec, P.; Smieskova, A.; Zidek, Z.; Zubek, M.; Schneider, P.; Kocirik, M.; Kozankova, J. Adsorption properties of ZSM-5 zeolites. *Collection of Czechoslovak Chemical Communications* **1998**, *63*, 141-154.
15. Sing, K. Reporting physisorption data for gas/solid systems. *Pure Appl. Chem.* **1982**, *54*, 2201-2218.
16. Müller, U.; Unger, K. K. Sorption studies on large ZSM-5 crystals: the influence of aluminium content, they type of exchangeable cations and the temperature of nitrogen hysteresis effects. *Stud. Surf. Sci. Catal.* **1988**, *39*, 101-108.
17. Delidovich, I.; Palkovits, R. Fructose production *via* extraction-assisted isomerization of glucose catalyzed by phosphates. *Green Chem.* **2016**, *18*, 5822-5830.
18. Bérubé, M.; Dowlut, M.; Hall, D. G. Benzoboroxoles as efficient glycopyranoside-binding agents in physiological conditions: structure and selectivity of complex formation. *J. Org. Chem.* **2008**, *73*, 6471-6479.
19. Dowlut, M.; D. G. Hall. An improved class of sugar binding boronic acids, soluble and capable of complexing glycosides in neutral water. *J. Am. Chem. Soc.* **2006**, *128*, 4226-4227.
20. Nicholls, M. P.; Paul, P. K. C. Structures of carbohydrate-boronic acid complexes determined by NMR and molecular modelling in aqueous alkaline media. *Org. Biomol. Chem.* **2004**, *2*, 1434-1441.
21. Van der Berg, R.; Peters, J. A.; Van Bekkum, H. The structure and (local) stability constants of borate esters of mono- and di-saccharides as studied by ^{11}B and ^{13}C NMR spectroscopy. *Carbohydr. Res.* **1994**, *253*, 1-12.

22. Karpa, M. J.; Duggan, P. J.; Griffin, G. J.; Freudigmann, S. J. Competitive transport of reducing sugars through a lipophilic membrane facilitated by aryl boron acids. *Tetrahedron* **1997**, *53*, 3669-3678.
23. Pham, T. N.; Samikannu, A.; Rautio, A-R.; Juhasz, K. L.; Konya, Z.; Wärna, J.; Kordas, K.; Mikkola, J-P. Catalytic hydrogenation of D-Xylose over Ru decorated carbon foam catalyst in a SpinChem® rotating bed reactor. *Top. Catal.* **2016**, *59*, 1165-1177.
24. Dietrich, K.; Hernández-Mejia, C.; Verschuren, P.; Rothenberg, G.; Shiju, N. R. One-pot selective conversion of hemicellulose to xylitol. *Org. Process Res. Dev.* **2017**, *21*, 165-170.
25. Ennaert, T.; Feys, S.; Hemdriks, D.; Jacobs, P. A.; Sels, B. F. Reductive splitting of hemicellulose with stable ruthenium-loaded USY zeolites. *Green Chem.* **2016**, *18*, 5295-5304.
26. Murzin, D. Y.; Kusema, B.; Murzina, E. V.; Aho, A.; Tokarev, A.; Boymirzaev, A. S.; Wärna, J.; Dapsens, P. Y.; Mondelli, C.; Pérez-Ramírez, J.; Salmi, T. Hemicellulose arabinogalactan hydrolytic hydrogenation over Ru-modified H-USY zeolites. *J. Catal.* **2015**, *330*, 93-105.
27. Ribeiro, L. S.; Delgado, J. J.; Órfão, J. J. M.; Pereira, M. F. R. A one-pot method for the enhanced production of xylitol directly from hemicellulose (corn cob xylan). *RSC Adv.* **2016**, *6*, 95320-95327.
28. Ribeiro, L. S.; Órfão, J. J. M.; Pereira, M. F. R. Screening of catalysts and reaction conditions for the direct conversion of corn cob xylan to xylitol. *Green Process. Synth.* **2017**, *6*, 265-272.

29. Ribeiro, L. S.; Órfão, J. J. M.; Pereira, M. F. R. Simultaneous catalytic conversion of cellulose and corncob xylan under temperature programming for enhanced sorbitol and xylitol production. *Bioresource Technol.* **2017**, *244*, 1173-177.
30. Irmak, S.; Canisag, H.; Vokoun, C.; Meryemoglu, B. Xylitol production from lignocellulosics: Are corn biomass residues good candidates? *Biocatal. Agric. Biot.* **2017**, *11*, 220-223.
31. Tathod, A. P.; Dhepe, P. L. Efficient method for the conversion of agricultural waste into sugar alcohols over supported bimetallic catalysts. *Bioresource Technol.* **2015**, *178*, 36-44.
32. Kobayashi, H.; Yamakoshi, Y.; Hosaka, Y.; Yabushita, M.; Fukuoka, A. Production of sugar alcohols from real biomass by supported platinum catalyst. *Catal. Today.* **2014**, *226*, 204-209.
33. Elliot, D. C.; Peterson, K. L.; Muzatko, D. S.; Alderson, E. V.; Hart, T. R.; G. G. Neuenschwander. Effects of trace contaminants on catalytic processing of biomass-derived feedstocks. *Appl. Biochem. Biotech.* **2004**, *113-116*, 807-825.